GEOLOGY

Anthropocene rockfalls travel farther than prehistoric predecessors

10.1126/sciadv.1600969

Josh Walter Borella,[1]* Mark Quigley,[1,2] Louise Vick[1]

Human modification of natural landscapes has influenced surface processes in many settings on Earth. Quantitative data comparing the distribution and behavior of geologic phenomena before and after human arrival are sparse but urgently required to evaluate possible anthropogenic influences on geologic hazards. We conduct field and imagery-based mapping, statistical analysis, and numerical modeling of rockfall boulders triggered by the fatal 2011 Christchurch earthquakes (n = 285) and newly identified prehistoric (Holocene and Pleistocene) boulders (n = 1049). Prehistoric and modern boulders are lithologically equivalent, derived from the same source cliff, and yield consistent power-law frequency-volume distributions. However, a significant population of modern boulders (n = 26) traveled farther downslope (>150 m) than their most-traveled prehistoric counterparts, causing extensive damage to residential dwellings at the foot of the hillslope. Replication of prehistoric boulder distributions using three-dimensional rigid-body numerical models that incorporate lidar-derived digital topography and realistic boulder trajectories and volumes requires the application of a drag coefficient, attributed to moderate to dense slope vegetation, to account for their spatial distribution. Incorporating a spatially variable native forest into the models successfully predicts prehistoric rockfall distributions. Radiocarbon dating provides evidence for 17th to early 20th century deforestation at the study site during Polynesian and European colonization and after emplacement of prehistoric rockfall. Anthropocene deforestation enabled modern rockfalls to exceed the limits of their prehistoric predecessors, highlighting a shift in the geologic expression of rockfalls due to anthropogenic activity. Reforestation of hillslopes by mature native vegetation could help reduce future rockfall hazard.

INTRODUCTION

The detachment of large rock particles from source cliffs and subsequent downslope displacement by bouncing and rolling (that is, rockfall) defines a major geologic hazard to humans and infrastructures in areas of steep topography (*1*, *2*). Rockfall spatial distributions are commonly mapped as part of geologic hazard assessments (*3*–*5*) and are often used to delineate areas of comparably high hazard on the premise that the past is the key to the future. However, deforestation of hillslopes can induce rapid landscape transformation (*6*, *7*) and may increase the exposure of humans, dwellings, and critical infrastructures to slope hazards including rockfalls, landslides, and debris flows (*8*, *9*). Understanding the impact of changing land cover conditions on rockfall distributions and hazard requires a thorough understanding of landscape evolutionary chronology, boulder distribution statistics and depositional age, and boulder trajectory from source to resting position. Here, we conduct these analyses in unprecedented detail.

Severe deforestation has accompanied anthropogenic colonization of natural landscapes in many settings globally (*7*, *10*), including New Zealand, where rapid deforestation began with Polynesian (Māori) settlement ca. 1280 CE and continued with European colonization from ca. 1800 CE (*11*–*13*). By 1900 CE, more than 98% of indigenous forests had been removed for urban and agricultural development in Banks Peninsula on the eastern coast of the South Island (Fig. 1, A to D) (*14*, *15*). Human activity was accompanied by marked floral and faunal changes (*11*, *16*), increased catchment erosion and alluvial sedimentation, and changes in river dynamics, marking the progressive emergence of the Anthropocene era (*13*, *17*–*20*).

[1]Department of Geological Sciences, University of Canterbury, Christchurch, Christchurch 8011, New Zealand. [2]School of Earth Sciences, The University of Melbourne, Parkville, Victoria 3010, Australia.
*Corresponding author. Email: josh.borella@pg.canterbury.ac.nz

Previous studies (*7*–*9*) have examined the influence of anthropogenic deforestation on increasing landslide frequency, but none specifically addressed its impact on rockfall hazard due to strong seismic-induced ground shaking. We are aware of no data that compare pre– with post–human arrival geologic phenomena with the resolution that we present in this study.

RESULTS

Here, we compare modern rockfall distributions and characteristics with their prehistoric counterparts at Rapaki in the Port Hills of southern Christchurch, New Zealand (Fig. 2, A to E). During the 22 February 2011 moment magnitude (M_w) 6.2 Christchurch earthquake (*21*), more than 6000 rockfall boulders were dislodged from source cliffs and deposited downslope, resulting in five fatalities, impacts to more than 200 homes, and widespread evacuations in the Port Hills (*22*). More than 400 individual rocks (285 within the study area) were dislodged from the volcanic source rock near the top of Mount Rapaki (Figs. 2A and 3) in the 22 February and 13 June 2011 earthquakes. Twenty-six of these rocks, ranging in volume from ~0.25 to ~28.0 m^3, affected the Rapaki village. Boulders traveled up to 770 ± 15 m downslope from the source cliff (Fig. 2, A and C).

During field mapping of modern rockfall at the Rapaki study site, abundant prehistoric rockfall boulders were discovered. The Global Positioning System location, elevation, volume, and lithology type were determined for 1049 individual prehistoric boulders with volume ≥0.1 m^3 (Fig. 2B). Prehistoric boulders are partially buried in colluvium and exhibit a high degree of surface roughness and lichen cover (Fig. 4), indicating long hillslope residence time. The absence of remobilization during the Canterbury earthquake sequence (CES) and the

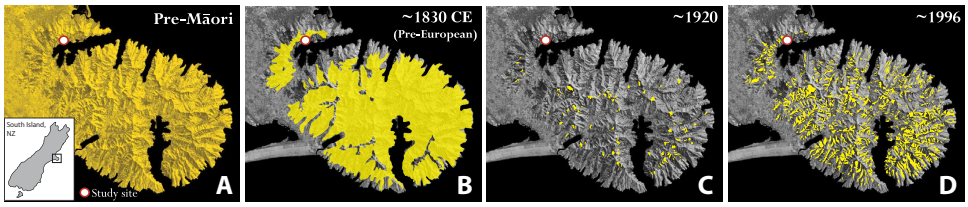

Fig. 1. Anthropogenic deforestation of Banks Peninsula. Removal of native forest (yellow) occurred rapidly in Banks Peninsula with the arrival of Polynesians (ca. 1280 CE) then Europeans (ca. 1830 CE). (**A**) Before arrival of the Polynesians (Māori), extensive native forest was present throughout Banks Peninsula. (**B**) Before European settlement, minor to moderate removal of indigenous forest by Māori had occurred in Banks Peninsula. Burning was the primary tool for clearance. (**C**) By 1920, Europeans had removed >98% of the native forest in Banks Peninsula, leaving slopes barren and low-lying areas vulnerable to slope hazards. (**D**) Minor reestablishment of old-growth native forest has occurred, but slopes in Banks Peninsula and the Port Hills (including Rapaki) remain largely unvegetated [data from previous studies (*14*–*16*)].

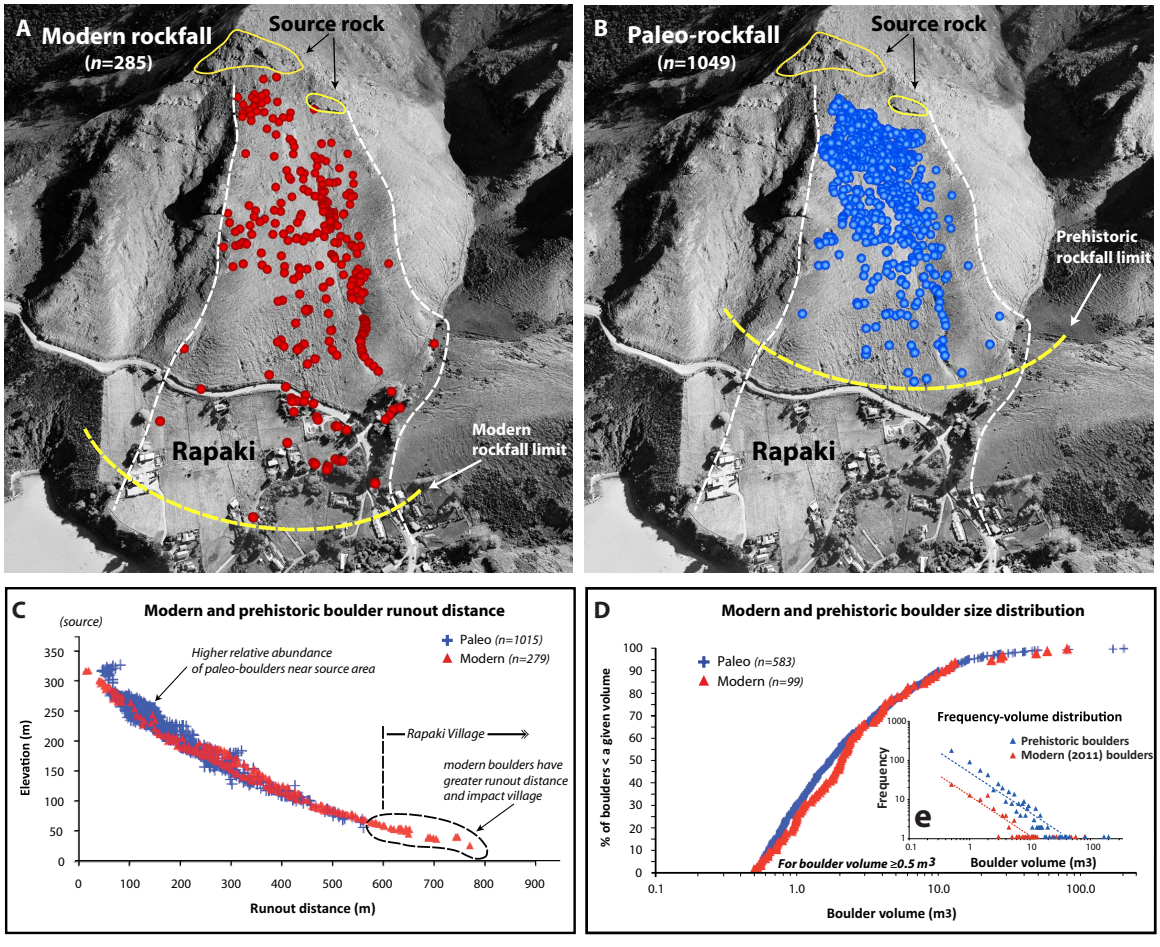

Fig. 2. Spatial distribution and size comparison of modern and prehistoric rockfall at Rapaki. (**A**) Spatial distribution for mapped modern rockfall (n = 285) generated during the 2011 Christchurch earthquakes (22 February and 13 June events). Twenty-six modern boulders affected the Rapaki village and caused severe damage to residential properties. Maximum runout distance (map length) for modern boulders is ~770 m. (**B**) Spatial distribution for mapped paleoboulders (n = 1049). No evidence for prehistoric boulders in area now occupied by the Rapaki village. Maximum travel distance for prehistoric boulders is ~560 m. (**C**) Modern and prehistoric rockfall runout distance plotted as function of elevation. Travel distance for modern rockfalls exceeds limit of prehistoric predecessors. (**D**) Comparison of boulder size distribution for modern and prehistoric boulders indicates strong similarity. (**E**) The frequency-volume distributions for prehistoric and modern rockfall at Rapaki show a similar power-law trend.

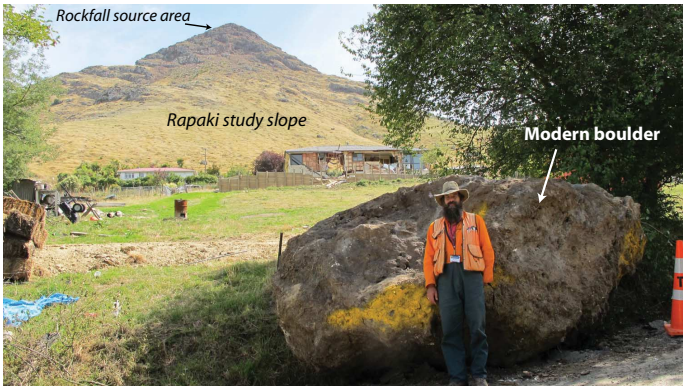

Fig. 3. Modern boulder at Rapaki study site. Photo of large modern boulder (~28 m^3) detached from Mount Rapaki and emplaced in the Rapaki village during the 22 February 2011 earthquake (photo courtesy of D. J. A. Barrell, GNS Science). The boulder traveled through the center of the residential home located in background (center). Boulder runout distance from source was ~700 m. Runout distance for furthest traveled modern boulders is significantly greater (~150 to 175 m) than travel distance for prehistoric boulders.

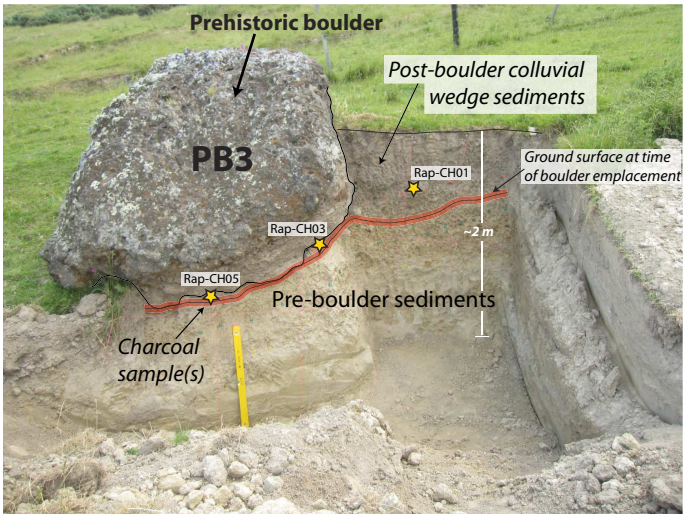

Fig. 4. Prehistoric boulder at Rapaki study site. Photo of exploratory trench excavated adjacent to Paleo-Boulder 3 (PB3), exposing hillslope sediments deposited before and after boulder emplacement. Locations for charcoal samples (yellow) Rap-CH01, Rap-CH03, and Rap-CH05 are shown. All samples were collected near the base of the most recent loess colluvial wedge sediments and yield similar conventional radiocarbon ages (203 ± 18, 197 ± 17, 222 ± 17 yr B.P., respectively). 2σ-Calibrated ages suggest a probable burning event occurred at Rapaki sometime between 1661 CE and 1950 CE, with highest 2σ subinterval probability between 1722 CE and 1810 CE. PB3 is deposited in footslope position, and volume is ~14.5 m^3. Total travel distance for PB3 is ~560 m.

accumulation of thick colluvial wedges behind sampled prehistoric boulders imply that boulders remained static after deposition. ^{3}He cosmogenic nuclide exposure ages (*23*) and preliminary optically stimulated luminescence dating (*24*) indicate that prehistoric rockfall was emplaced no earlier than ~3 to 6 ka (thousand years ago), long before the arrival of Polynesians (Māori) and Europeans.

The prehistoric rockfall is attributed to a strong proximal earthquake at ca. 6 to 8 ka (*23*). The lack of any significant rockfall created at Rapaki during the 4 September 2010 main shock, 23 December 2011 aftershock, recent (14 February 2016) M_w 5.7 Valentine's Day earthquake, or estimated 1:100-year intensity storms in April 2014 suggests that most of the source rock is not "waiting to fall" but rather requires a significant stress for detachment of rock bodies (*23*). This is further supported by the absence of any prehistoric rockfall dated before ~3 to 6 ka (*23*, *24*), implying that higher-frequency precipitation events do not generate extensive rockfall. The Rapaki source rock is not (and would not have been for at least the past ~30 ka) located directly adjacent to any rivers or the harbor coastline, thereby eliminating natural undercutting as a potential triggering mechanism, and, even during the last glacial maximum (~24 to 18 ka), would have obtained an elevation of only ~500 to 520 m above sea level, precluding it from sustained freeze-thaw conditions (that is, high precipitation and temperature fluctuations), typical in high mountainous elevations (for example, Southern Alps).

Comparison of modern and prehistoric boulder spatial distributions (Fig. 2, A and B) indicates that (i) both have increased concentrations in topographic lows, (ii) both have decreased concentrations on interfluves, (iii) prehistoric boulders have shorter maximum runout distances (560 ± 15 m) compared to modern, and (iv) prehistoric rockfall is more concentrated near the source area compared to modern (Fig. 2C). A Kolmogorov-Smirnov (KS) comparison test confirms the lack of similarity between modern and prehistoric boulder spatial distributions and indicates that the maximum difference between cumulative distributions is 0.636 with a corresponding low P value of 0.012 (see Materials and Methods for details of KS test and data S1). No prehistoric boulders were identified on the surface or in the shallow subsurface in the area now occupied by the Rapaki village from field mapping and inspection of historical aerial photographs dating back to 1926. In interviews with the local Māori, they indicated, based on a review of their recorded oral history, that there are no accounts of large boulders being removed or repositioned by their ancestors in the Rapaki village area.

Modern and prehistoric boulders are lithologically equivalent and maintain consistent frequency volume distributions (Fig. 2, D and E). Statistical coherence is observed at 25th percentile (modern, 1.01 m^3; prehistoric, 0.89 m^3), median (modern, 2.05 m^3; prehistoric, 1.70 m^3), and 75th percentile (modern, 4.16 m^3; prehistoric, 4.53 m^3) boulder sizes. KS analysis indicates a maximum difference between cumulative distributions of 0.102 with a corresponding P value of 0.326 (see data S2). Similarities in boulder shape and size exist because the prehistoric and modern rockfalls at Rapaki are sourced from the same parent rock, where jointing in the source rock, predominantly from early cooling of the lava flows, imparts a first-order control on boulder size and shape. Given its probable early formation and the persistent nature of jointing within the volcanic source rock, it is reasonable to assume that joint control on boulder size and shape has remained constant over time (that is, during multiple rockfall events). The abundance of both modern and prehistoric boulders in the same topographic lows suggests that slope characteristics have also remained relatively constant with time and that, from a landscape evolution perspective, the time between rockfall events (~3000 to 7000 years) and that recorded by all observable rockfall (both prehistoric and modern) (estimated at ~25,000 years) at Rapaki is relatively short. It is difficult to determine the influence that previous boulders might have had on changing the runout path for subsequent rockfall deposits. We expect

that impacts could be common near the source cliff but much less so at midslope and footslope positions, because the frequency of boulders declines rapidly (power law reduction) and diffusion increases with increasing distance from the source area. If accumulated debris were an important limit on rockfall extents, we would predict a reduction of modern boulder runout distances with increasing time rather than the observed increase, due to an increased likelihood of boulder impacts with increasing hillslope debris. In addition, we cannot dismiss outright that potential collisions of traveling boulders with other mobile rockfall debris could have influenced rockfall runout distances in some cases (*25*) but assume that the impact of this effect would be of similar extent during all major rockfall events and relatively unimportant given the steep slopes and rapid boulder velocities during transport (Fig. 5, A and C).

Given the similarities in lithology and morphology but differences in runout distances between the modern and prehistoric boulder data sets, the abundance of evidence suggesting the presence of a dense native forest on in Banks Peninsula hillslopes during prehistoric times, and the observation that contemporary boulder impacts with trees were observed frequently in other (forested) parts of the landscape after the Christchurch earthquakes, it is sensible to reason that prehistoric boulder runouts may have been impeded by natural vegetation at the study site before deforestation. To test this hypothesis, we used rapid mass movement simulation (RAMMS) software (*26*–*28*) and a 3-m DEM (digital elevation model) derived from post-earthquake LIDAR (light detection and ranging) surveys to model modern and prehistoric rockfall distributions. Boulder trajectories and bounce positions were reconstructed using ground mapping and 10-cm resolution aerial photography. A total of 700 boulders with power-law frequency-volume distributions were released from three separate source rock areas (Fig. 5, A and C) (see Materials and Methods); rockfall source areas and partitioning of boulder volumetric flux were informed by field observations from the 2011 Christchurch earthquakes.

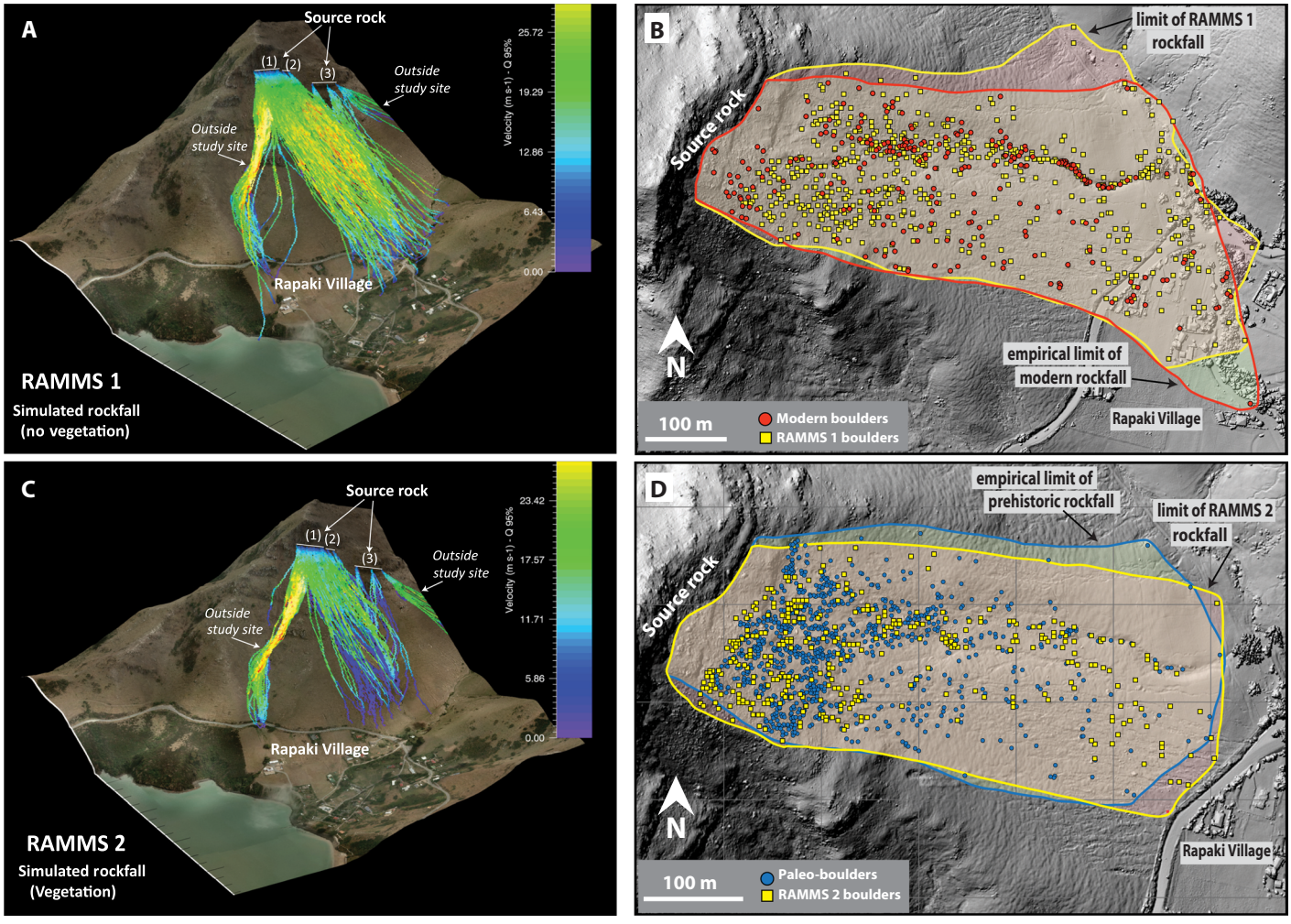

Fig. 5. RAMMS rockfall modeling. (**A**) Simulated rockfall assuming no hillslope vegetation (RAMMS 1). Source areas, rockfall trajectories, boulder velocities, and final resting positions are shown. (**B**) RAMMS 1 successfully predicts modern boulder distributions, highlighting effectiveness of RAMMS in replicating modern rockfall distribution. (**C**) Simulated rockfall assuming moderate to dense vegetation on the hillslope (RAMMS 2). Vegetation is modeled in RAMMS as forest drag, a resisting force that acts on the rock's center of mass when located below the drag layer height. The forest is parameterized by the effective height of the vegetation layer (10 m) and a drag coefficient (moderate, 3000 kg/s; dense, 6000 kg/s). (**D**) Prehistoric and RAMMS 2 boulder distributions display strong correlation, suggesting that a moderate to dense forest likely existed on the Rapaki hillslope during prehistoric boulder deposition.

RAMMS 1 (modern unvegetated landscape model) yields spatial distributions and maximum runout distances (700 to 770 m) for simulated boulders that overlap tightly with empirical modern rockfall distributions (Figs. 5B and 6). The percentage of RAMMS 1 boulders deposited near the source rock (shadow angles 32° and 33°) is <25%. KS analysis indicates high correlation (P = 0.736) between RAMMS 1–simulated boulders and empirical data (see data S3), highlighting the ability of RAMMS to successfully replicate rockfall trajectories and runouts. RAMMS 1 significantly overpredicts prehistoric rockfall runout distance and underpredicts near-source prehistoric rockfall relative frequency. KS analysis between RAMMS 1 and prehistoric boulders yields a low P value of 0.012 (see data S4). Given the probable middle Holocene age of prehistoric rockfalls, we explored whether changes in the impact of slope vegetation between modern and prehistoric rockfalls could account for differences in respective boulder spatial distributions.

We implemented spatially variable, moderate to dense native hillslope vegetation (modeled using a forest drag coefficient) into RAMMS simulations (RAMMS 2) to test whether more accurate replication of prehistoric boulders could be achieved with forest cover. Before the Polynesian and European settlement, Banks Peninsula was almost completely covered by a richly varied native forest (Fig. 1A) (*15*, *29*–*31*). Warm-temperate and frost-sensitive species like nikau palm and akeake grew in coastal gully forests, whereas valley floors and lower slopes were covered by tall podocarp forests dominated by kahikatea, lowland totara, and matai (*15*, *29*). Pollen and phytolith analyses from core samples taken in Banks Peninsula (Gebbies Pass) are consistent with the presence of a podocarp forest during the Holocene and persistent woody conditions even in cooler glacial periods (*30*, *31*). Therefore, it is reasonable to assume that similar forest conditions existed on the Rapaki hillslope before deforestation.

RAMMS 2 boulders show the highest volumetric proportions (~62 to 64% of total population) near the source rock at steep (33°) shadow angles (that is, angle from the horizontal of a line projected from the source area base to the top of a runout boulder) and increased volumes in the northern drainage gulley, consistent with distributions of mapped prehistoric boulders (Figs. 5D and 6). Boulder frequency decreases with increasing distance from the source rock and on the southern middle to lower-slope interfluve. The maximum modeled boulder runout distance is ~560 to 600 m. No RAMMS 2 boulders reach the Rapaki village. A KS comparison test between prehistoric rockfall and RAMMS 2 boulders indicates high correlation, with a P value of 0.736 (see data S5). We conclude that the dense native forest cover increased the frequency of boulder-forest impacts and increased frictional drag on boulders during rockfall events, thereby limiting runout distances.

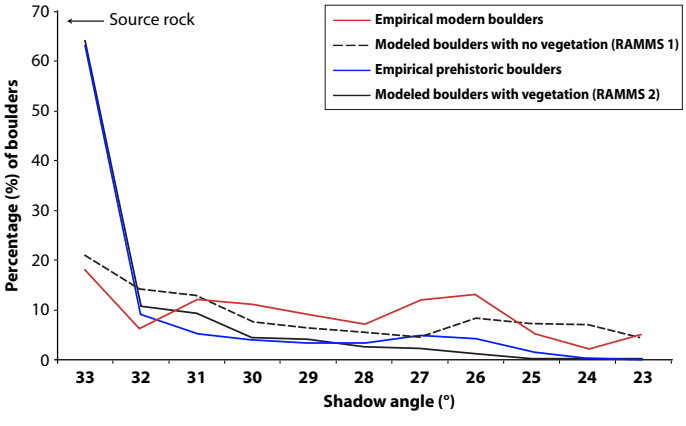

Fig. 6. Comparison of empirical and modeled rockfall spatial distributions. Empirical prehistoric and RAMMS 2 boulders (vegetation) display a strong similarity (P = 0.736) with the highest frequency (~62 to 64%) of boulders near the source rock (shadow angle 33°). Empirical modern and RAMMS 1 boulders (no vegetation) show an equivalently high correlation (P = 0.736). In contrast, mapped prehistoric and modern boulders display a poor fit (P = 0.012). ArcGIS has been used to determine percentage of boulders within each shadow angle.

Radiocarbon dating of charcoal found within loess colluvium sediments at the study site suggests removal of native forest by burning occurred sometime between 1661 CE and 1950 CE (2σ-calibrated age), marking its occurrence well after deposition of prehistoric rockfall (see Table 1 and Fig. 4) (*6*–*8*) and sometime during the Māori and subsequent European occupation. Although we cannot exclude natural fire as a mechanism for deforestation, the onset of increased colluvial sedimentation during the period of local human colonization, widespread evidence for anthropogenic deforestation elsewhere in the region, and absence of modern forest cover suggest anthropogenic sustainment of an unforested landscape since the 17th to earliest 20th century. Anthropogenic landscape modification between successive rockfall-triggering events enabled modern rockfall runout distances to exceed the identified limits of their prehistoric predecessors, providing geologic evidence for the emergence of the Anthropocene (Fig. 7).

DISCUSSION

The 2011 Christchurch earthquakes provide the rare opportunity to map the distribution and trajectory of modern rockfall deposits and compare them to prehistoric predecessors. We attribute the discrepancy between spatial distributions of modern and prehistoric rockfall deposits identified in this study to intervening landscape change in the form of Anthropocene deforestation sometime between 1661 CE and 1950 CE. Field mapping (Fig. 8, A to C) suggests that increased modern rockfall runout distance occurred in other deforested areas of the Port Hills (Banks Peninsula), highlighting the widespread impact that removal of native forest has on increasing rockfall hazard. Deforestation allowed modern boulders to travel further than their geologic predecessors and damage infrastructures in downslope areas at source distances beyond what would be predicted from the distribution of past rockfall deposits (see Figs. 2, A to C, and 8, A and C). Increases in hillslope substrate wetness relating to climate change or short-term weather fluctuations could theoretically reduce hillslope frictional properties and increase rockfall runout distances due to elevated substrate pore pressures. However, this potential effect seems unimportant in this area because paleoclimate models (*32*) suggest cooler and wetter mid-Holocene (ca. 6000 yr B.P.) climates in eastern New Zealand relative to present, which should have favored longer prehistoric rockfall runout distances relative to modern distances, in opposition to what we observe.

Assessments of rockfall hazard must consider the potential for future effects to surpass prehistoric geologic analogs in severity and extent, particularly where intervening anthropogenic activity has

Table 1. Results from radiocarbon dating of charcoal within loess colluvium sediments at Rapaki, New Zealand. NZA, Rafter Radiocarbon Laboratory; ^{14}C yr B.P., radiocarbon years before the present.

Sample ID	Exposure unit	NZA laboratory number	$\delta^{13}C$	Radiocarbon age	Calibrated age 2σ	Probability for each 2σ range	Materials and significance
				(^{14}C yr B.P.)	(Calendar year CE)	(%)	
Rap-CH01	Loess colluvium	56801	−28.6 ± 0.2	203 ± 18	1664–1698, 1724–1809, 1870–1876	22.8, 70.4, 1.0	Charcoal in colluvial wedge sediment. Dates probable burning event at Rapaki.
Rap-CH03	Loess colluvium	56802	−29.1 ± 0.2	197 ± 17	1666–1700, 1722–1810, 1838–1845, 1867–1878, 1933–1938, 1946–1950	25.8, 63.8, 1.3, 2.4, 0.6, 1.1	Charcoal in colluvial wedge sediment. Dates probable burning event at Rapaki.
Rap-CH05	Loess colluvium	56803	−27.9 ± 0.2	222 ± 17	1661–1680, 1732–1802	15.8, 79.0	Charcoal in colluvial wedge sediment. Dates probable burning event at Rapaki.

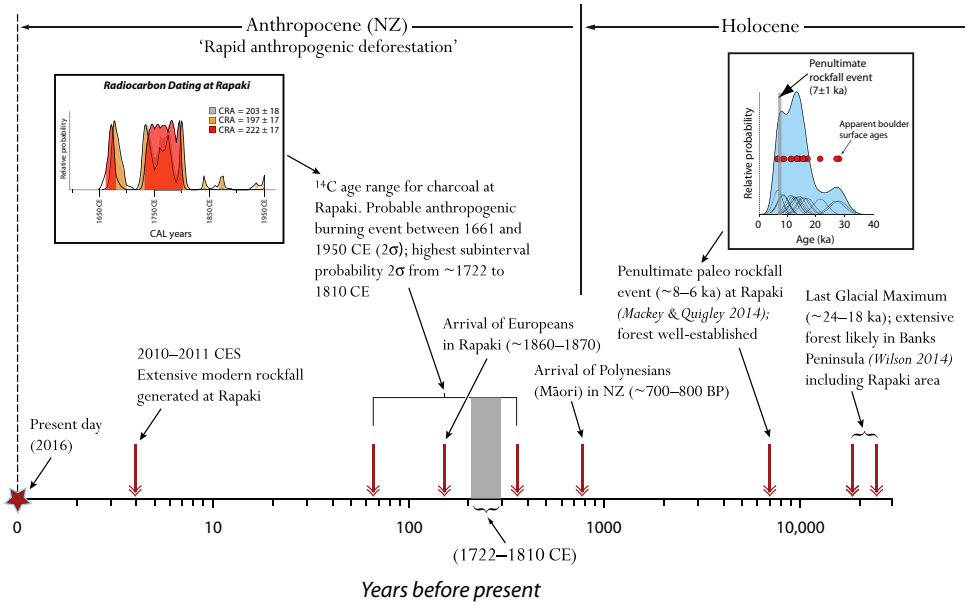

Fig. 7. Rockfall and Anthropocene chronology for Rapaki study site. Native forest likely persisted during the Last Glacial Maximum and thrived during the Holocene in Banks Peninsula and at Rapaki. The penultimate paleorockfall event at Rapaki occurred approximately 8 to 6 ka [taken from the study of Mackey and Quigley (*23*)] when a dense variable forest cover would have existed on the hillslope. Radiocarbon dating of charcoal at Rapaki suggests a probable burning event occurred sometime between 1661 CE and 1950 CE, with highest subinterval probability between 1722 CE and 1810 CE. Slope deforestation by Māori and later Europeans allowed modern rockfall generated during the 2011 Christchurch earthquakes to travel further than their prehistoric predecessors and affected the Rapaki village.

modified the landscape (see Figs. 2, A to C, and 8, A and B). However, a positive implication of this study is that naturally regenerating native forest or exotic plantation forest (see Fig. 8B) cover may provide an effective and time-resilient method for mitigating rockfall hazard. The paleo–forest cover at Rapaki was presumably able to regenerate and dynamically stabilize itself through several high-impact rockfall events and changing climate (*23*, *24*) (that is, glacial to interglacial), essential capacities for any protective forest. Local and global discussions on the efficacy of forest cover (*33*, *34*) for mitigating rockfall hazard are becoming increasingly important as human settlement continues to expand into hilly and mountainous regions throughout the world.

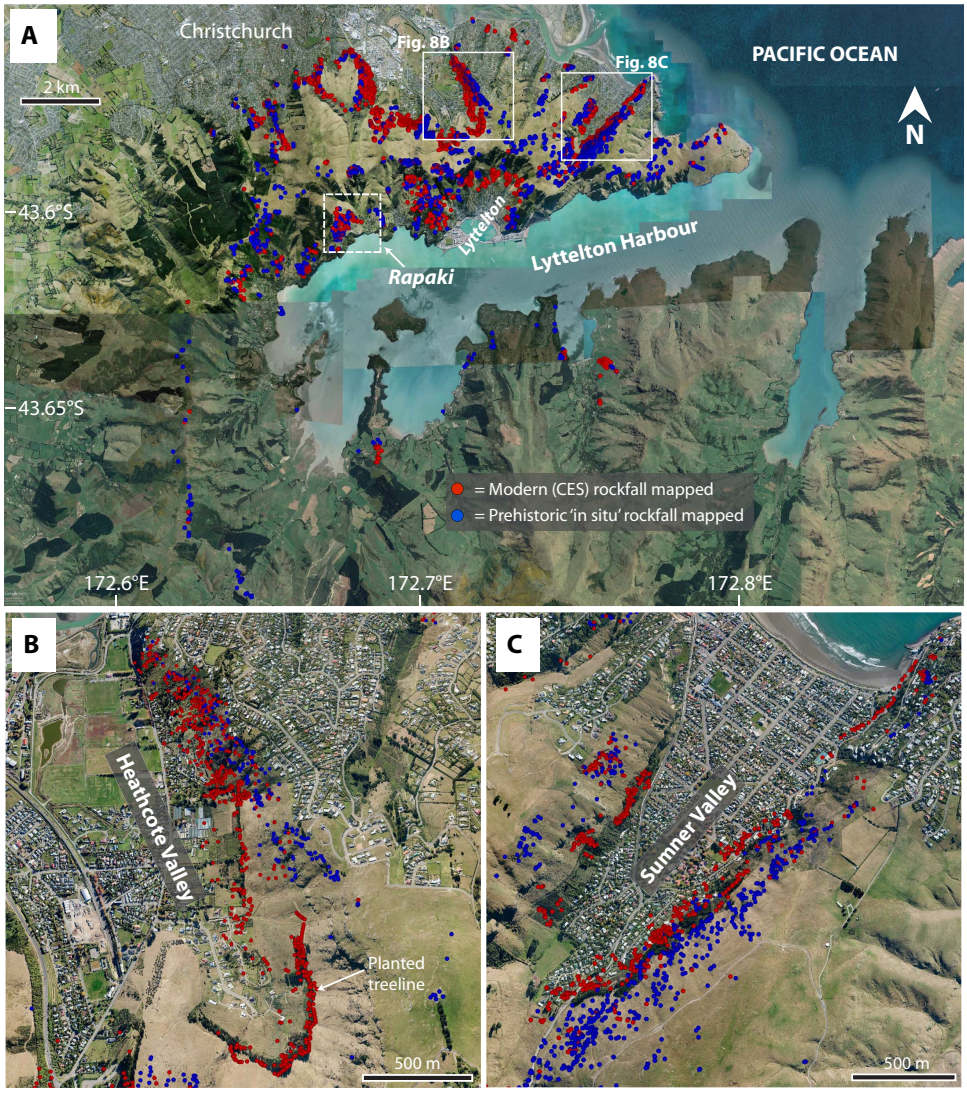

Fig. 8. Comparison of spatial distribution for modern (CES) and prehistoric rockfall in Port Hills of southern Christchurch. (**A**) Mapped modern (red) and prehistoric (blue) "in situ" rockfall. Rockfall data shown have been provided by the Christchurch City Council and were mapped in the field by GNS Science. [Prehistoric rockfall was only partially mapped in certain areas, such as upslope of the planted treeline shown in (B). However, for areas adjacent to high-density residential development, both modern and prehistoric rockfalls appear well mapped, and comparison of boulder runout distances clearly highlights the increased travel distance for CES-generated boulders. Burial of preexisting boulders by colluvial and alluvial sediments is possible, particularly in the footslope position, and would limit the number of observable prehistoric rockfalls.] Slopes in the Port Hills have been stripped of native vegetation. (**B**) Comparison of CES-generated and prehistoric in situ rockfall in Heathcote Valley reveals longer runout distances (~150 to 250 m) for CES rockfall boulders. Modern rockfall affected numerous residential dwellings. The southern planted treeline was effective in capturing modern rockfall, highlighting the importance of slope vegetation in mitigating rockfall hazard. (**C**) Modern rockfall boulders on the northwestern and southeastern sides of Sumner Valley display further runout distances (~50 to 100 m) than in situ [we recognize the possibility that, in rare cases, isolated exposures of intact volcanic bedrock may be mapped as in situ (prehistoric) boulders] or preexisting rockfall.

MATERIALS AND METHODS

Mapping and characterization of prehistoric and modern rockfall boulders

We mapped 1543 individual prehistoric rockfall boulders at the Rapaki study site. Location (that is, latitude/longitude) and elevation (meters above sea level) were recorded for each rockfall deposit using a handheld Garmin GPSMAP 62s device. Boulder dimensions (that is, height, length, and width) were tape-measured in the field. For prehistoric boulders partially buried to the degree that only two dimensions were adequately measurable, the shorter of the two measured lengths was used for the third dimension, thus ensuring a conservative boulder size estimate. No rounding factor has been applied to volumetric estimations of prehistoric boulders. Mapped prehistoric rockfall size (volume) ranged from 0.001 to >100 m^3. However, a negative sample bias exists for rockfall deposits with volume <0.1 m^3. At lower and mid-slope elevations, prehistoric rockfall

deposits were mapped and recorded for the full-size range (0.001 to >100 m^3). At higher elevations, small rockfall populations (<0.1 m^3) were too high to be accurately mapped within a reasonable time frame. Consequently, the data set used for statistical analysis within our study was composed of prehistoric boulders with a volume ≥0.1 m^3 (n = 1049), thus ensuring no sample bias within the analyzed boulder volume data set. Because of safety concerns, prehistoric boulder volumes were not recorded within ~100 meters of the source rock. Lithology type was determined for each prehistoric boulder and was based primarily on the observed dominant rock "texture." Boulders were designated as either (i) volcanic breccia basalt or (ii) massive finely crystalline basalt. Transitional textures were occasionally observed in the field but are rare and represent outliers.

Collection of modern rockfall data reflects the combined efforts of L.V. (coauthor), Aurecon, and GNS. Three hundred seven individual modern boulders were identified in Rapaki. Because of safety concerns, 189 of the boulders were mapped via a geographic information system desktop study using post-earthquake high-resolution (10 cm) aerial photographs and therefore provided no boulder size data. Of the 118 modern boulders mapped in the field, 99 contain x-y-z length dimensions, thus providing a boulder volume. For comparison of modern and prehistoric boulder size distributions, all 99 of the recorded modern boulder volumes have been used. Modern boulder volumes were calculated by the lead author using Microsoft Excel. No rounding factor has been applied to the modern boulder sizes. L.V. used a similar criterion for description of the boulder lithology types, designating each as either (i) volcanic breccia basalt or (ii) massive lava.

Measuring runout distance for prehistoric and modern rockfall boulders

Boulder runout distance was analyzed by examining the distance from the nearest potential source area to their final resting position. Map- and ground-length runout distances were measured using Google Earth Pro along the best-estimated local fall line projected downslope perpendicular to the local contour line. Runout distance was calculated for 1049 prehistoric boulders and 279 modern boulders within the Rapaki study site. We report map-length runout distance.

Details and application of RAMMS rockfall model

RAMMS is a rigid-body three-dimensional rockfall simulation program (*26*, *35*). Terrain was modeled using a high-resolution DEM, and rocks were modeled as rigid polyhedra. The user imports rocks as point clouds or selects predefined rock shapes from the model library. The RAMMS boulder library contains three shapes: equant (equidimensional), flat (one short axis and two long axes), and long (two short axes and one long axis). Boulder shapes are generated from laser scans of real rocks, so that natural irregularity and angularity are incorporated. The rigid-body element of the model allows the influence of rock shape to affect the outcomes of the hazard assessment by incorporating natural variability in slope-block interactions (*26*, *28*). Rock interaction with the substrate in RAMMS is a function of "slippage" through near-surface material, defined by the user as a function of Coulomb friction and drag force (*26*, *28*). RAMMS developers argue that rockfall impacts with soil are not simple point rebounds (*26*, *35*), as usually described in rockfall models and quantified by coefficient of restitution. Instead, they are complex three-dimensional interactions with the substrate that include sliding a block through material until maximum frictional resistance is reached and angular momentum is generated by contact forces, which cause the block to be launched from the ground (*26*, *35*, *36*). The slippage can be parameterized for hard surfaces (for example, rock) by decreasing the distance and time spent during impact, to better reflect the instantaneous rebound observed in rock-rock interactions. RAMMS parameters were calibrated from modern (2010–2011) rockfall data and therefore inherently incorporate in-motion processes, such as boulder-boulder interaction. Any effect this process may have on boulder runout distance, dynamic properties, such as velocity and kinetic energy, and lateral spread of the deposit is considered during the calibration process by replicating the empirical modern boulder data set (*28*).

The source area was delineated as a polyline shapefile in ArcGIS from a desktop study of orthophotography and satellite imagery. Because it is not known from exactly which section of the source cliff the prehistoric boulders were released, the entire source cliff was delineated. Three separate source rock areas were used (Fig. 2, A and B) and have been weighted differently based on our field observations of the source rock conditions and relative frequency of modern rockfalls detached from each source area during the 2011 Christchurch earthquakes. For approximately every nine boulders released from area 1, a single boulder is released from areas 2 and 3. A reduction in the number of boulders released from areas 2 and 3 was accomplished by creating less release points along these source lines. The number of release points is 35, with 20 boulders released from each source (seeder) point, making the initial total boulder count 700.

Boulder shape and size are highly influential in the dynamics and runout of a rockfall event (*28*, *35*, *37*). Boulder shapes and sizes used in the model simulations were representative of the true boulder geometries. Here, a virtual boulder population was created, using the RAMMS "rock builder" tool, which creates boulder point clouds based on a user-defined shape and size. The sizes in this case were chosen from statistical analysis of the paleo–boulder inventory, which includes volume estimated from axis proportions. We assumed a power-law distribution for the frequency-volume of simulated boulders, consistent with prehistoric boulders at Rapaki (power-law equation: $y = 83.607x^{-1.242}$, $R^2 = 0.86$). The following percentages have been attributed to each boulder size range within RAMMS: ~60% for 0.1 to 1 m^3, ~35% for 1 to 10 m^3, and ~5% for 10 to 100 m^3. For each size class of boulder, varying shapes were selected, which are simplified to equant, flat, and long. Twenty boulders were created with varying shapes, sizes, and densities (relative proportions of volcanic breccia and massive lava densities were applied).

Vegetation was modeled in RAMMS as forest drag, a resisting force that acts on the rock's center of mass when located below the drag layer height. The forest was parameterized by the effective height of the vegetation layer and a drag coefficient. Typical values for this coefficient ranged between 1000 and 10,000 kg/s (*26*, *35*). A variable forest density was applied to account for the presumed denser vegetation within the northern drainage valley at the Rapaki study site. We assumed that more surface and subsurface water would be focused into the northern drainage gully and would therefore promote denser tree growth. Within the drainage gulley, a uniform drag force of 6000 kg/s was applied to each of the simulated boulders. Elsewhere on the hillslope, a drag force of 3000 kg/s was applied. As evidenced by modern native forest analogs, tree growth was extended upward to the base of the source rock, and an average tree height of 10 m was used within the RAMMS model.

Simulation results were analyzed as ArcGIS shapefiles, and boulder numbers within each rockfall shadow zone were summed for comparison to the mapped modern and prehistoric boulder distributions. For each shadow zone (23° to >30°), the percentage of deposited simulated boulders was compared to the percentage of empirical boulders (that is, modern or prehistoric) within the zone for quantitative analysis of the down-slope distribution. Shadow zones were created on the basis of Evans and Hungr (*1*) rockfall shadow angle (that is, the angle from the horizontal of a line projected from the base of the source area to the top of the runout boulder). By combining this concept and the viewshed tool in ArcGIS, a series of shadow angle contours can be created, with 23° being the maximum runout distance achieved locally during the 2010–2011 CES.

KS test

We used the KS test to quantify the "goodness of fit" between two data sets (*38*). The two-sample KS test is a nonparametric, distribution-free method that uses the maximum vertical deviation between the empirical distribution functions (D) of two samples (for example, curves) to generate a corresponding P value. If the P value is >0.05, then the null hypothesis of no significant difference between two measured phenomena is not rejected. A P value equal to 1 reflects identical data sets. See data S1 to S4 for individual KS tests performed on Rapaki rockfall data.

Radiocarbon dating

Charcoal samples for radiocarbon dating were retrieved from colluvial wedge sediments accumulated at the backside of PB3 (fig. S2). Samples were dried at 40°C for 1 week and then sorted to separate the organic material from the host sediment. Between 70- and 500-mg samples of charcoal were submitted to the Rafter Radiocarbon Laboratory in Wellington, New Zealand, for accelerator mass spectrometry radiocarbon analysis. Samples were further cut and scraped with a scalpel at the Rafter Laboratory to remove any remaining surface dirt. Chemical pretreatment was done by repeated acid and alkali treatment. The weight obtained after chemical pretreatment ranged between 21.9 and 45.2 mg. Carbon dioxide was generated by elemental analyzer combustion, and 1 mg of C was obtained. Sample carbon dioxide was converted to graphite by reduction with hydrogen over iron catalyst. Conventional radiocarbon age (yr B.P.) is reported as defined by Stuiver and Polach (*39*). Ages were calibrated using the Southern Hemisphere calibration curve (SHCal13) (*40*). Radiocarbon ages referred to in the text are reported as 2σ calendar–calibrated age ranges (*41*). Detailed age range distributions of the calendar-calibrated ages are presented in table S1.

SUPPLEMENTARY MATERIALS

Supplementary material for this article is available at http://advances.sciencemag.org/cgi/content/full/2/9/e1600969/DC1

fig. S1. Radiocarbon calibration report for charcoal sample Rap-CH01.
fig. S2. Radiocarbon calibration report for charcoal sample Rap-CH03.
fig. S3. Radiocarbon calibration report for charcoal sample Rap-CH05.
data S1. KS comparison test of empirical prehistoric and modern boulders.
data S2. KS comparison test of frequency-volume distributions for modern and prehistoric boulders.
data S3. KS comparison test of empirical modern and RAMMS 1 boulders.
data S4. KS comparison test of empirical prehistoric and RAMMS 1 boulders.
data S5. KS comparison test of empirical prehistoric and RAMMS 2 boulders.

REFERENCES AND NOTES

1. S. G. Evans, O. Hungr, The assessment of rockfall hazard at the base of talus slopes. *Can. Geotech. J.* **30**, 620–636 (1993).
2. M. J. Selby, *Hillslope Materials and Processes* (Oxford Univ. Press, New York, ed. 2, 1993), 451 pp.
3. F. Guzzetti, P. Reichenbach, G. F. Wieczorek, Rockfall hazard and risk assessment in the Yosemite Valley, California, USA. *Nat. Hazards Earth Syst. Sci.* **3**, 491–503 (2003).
4. M. Jaboyedoff, V. Labiouse, Technical Note: Preliminary estimation of rockfall runout zones. *Nat. Hazards Earth Syst. Sci.* **11**, 819–828 (2011).
5. G. M. Stock, N. Luco, B. D. Collins, E. L. Harp, P. Reichenbach, K. L. Frankel, *Quantitative Rock-Fall Hazard and Risk Assessment for Yosemite Valley, Yosemite National Park, California* (U.S. Geological Survey Scientific Investigations Report 2014–5129, 2014), 52 pp.
6. E. F. Lambin, B. L. Turner, H. J. Geist, S. B. Agbola, A. Angelsen, J. W. Bruce, O. T. Coomes, R. Dirzo, G. Fischer, C. Folke, P. S. George, K. Homewood, J. Imbernon, R. Leemans, X. Li, E. F. Moran, M. Mortimore, P. S. Ramakrishnan, J. F. Richards, H. Skånes, W. Steffen, G. D. Stone, U. Svedin, T. A. Veldkamp, C. Vogel, J. Xu, The causes of land-use and land-cover change: Moving beyond the myths. *Glob. Environ. Chang.* **11**, 261–269 (2001).
7. D. B. McWethy, C. Whitlock, J. M. Wilmshurst, M. S. McGlone, M. Fromont, X. Li, A. Dieffenbacher-Krall, W. O. Hobbs, S. C. Fritz, E. R. Cook, Rapid landscape transformation in South Island, New Zealand, following initial Polynesian settlement. *Proc. Natl. Acad. Sci. U.S.A.* **107**, 21343–21348 (2010).
8. T. Glade, Landslide occurrence as a response to land use change: A review of evidence from New Zealand. *Catena* **51**, 297–314 (2003).
9. M. Guns, V. Vanacker, Shifts in landslide frequency–area distribution after forest conversion in the tropical Andes. *Anthropocene* **6**, 75–85 (2014).
10. F. Achard, H. D. Eva, H.-J. Stibig, P. Mayaux, J. Gallego, T. Richards, J.-P. Malingreau, Determination of deforestation rates of the world's humid tropical forests. *Science* **297**, 999–1002 (2002).
11. J. S. Harding, Historic deforestation and the fate of endemic invertebrate species in streams. *N. Z. J. Mar. Freshwater Res.* **37**, 333–345 (2003).
12. M. S. McGlone, Polynesian deforestation of New Zealand: A preliminary synthesis. *Archaeol. Oceania* **18**, 11–25 (1983).
13. I. C. Fuller, M. G. Macklin, J. M. Richardson, The geography of the Anthropocene in New Zealand: Differential river catchment response to human impact. *Geogr. Res.* **53** 255–269 (2015).
14. W. B. Johnston, *Locating the Vegetation of Early Canterbury: A Map and the Sources* (Transactions of the Royal Society, New Zealand, 1961), vol. 1, pp. 5–15.
15. H. D. Wilson, *Plant Life on Banks Peninsula* (Manuka Press, Cromwell, 2013).
16. C. J. Burrows, Fruit, seeds, birds and the forests of Banks Peninsula. *N. Z. Nat. Sci.* **21**, 87–108 (1994).
17. C. N. Waters, J. Zalasiewicz, C. Summerhayes, A. D. Barnosky, C. Poirier, A. Galuszka, A. Cearreta, M. Edgeworth, E. C. Ellis, M. Ellis, C. Jeandel, R. Leinfelder, J. R. McNeill, D. d. Richter, W. Steffen, J. Syvitski, D. Vidas, M. Wagreich, M. Williams, A. Zhisheng, J. Grivevald, E. Odada, N. Oreskes, A. P. Wolfe, The Anthropocene is functionally and stratigraphically distinct from the Holocene. *Science* **351**, aad2622 (2016).
18. J. Zalasiewicz, C. N. Waters, M. Williams, A. D. Barnosky, A. Cearreta, P. Crutzen, E. Ellis, M. A. Ellis, I. J. Fairchild, J. Grinevald, P. K. Haff, I. Hajdas, R. Leinfelder, J. McNeil, E. O. Odada, C. Poirier, D. Richter, W. Steffen, C. Summerhayes, J. P. M. Syvitski, D. Vidas, M. Wagreich, S. L. Wing, A. P. Wolfe, Z. An, N. Oreskes, When did the Anthropocene begin? A mid-twentieth century boundary level is stratigraphically optimal. *Quat. Int.* **383**, 196–203 (2015).
19. J. Zalasiewicz, M. Williams, A. Haywood, M. Ellis, The Anthropocene: A new epoch of geological time? *Philos. Trans. R. Soc. A* **369**, 835–841 (2011).
20. S. L. Lewis, M. A. Maslin, Defining the anthropocene. *Nature* **519**, 171–180 (2015).
21. C. I. Massey, M. J. McSaveney, T. Taig, L. Richards, N. J. Litchfield, D. A. Rhoades, G. H. McVerry, B. Lukovic, D. W. Heron, W. Ries, R. J. Van Dissen, Determining rockfall risk in Christchurch using rockfalls triggered by the 2010–2011 Canterbury Earthquake Sequence. *Earthq. Spectra* **30**, 155–181 (2014).
22. D. Heron, B. Lukovic, C. Massey, W. Ries, M. McSaveney, GIS modelling in support of earthquake-induced rockfall and cliff collapse risk assessment in the Port Hills, Christchurch. *J. Spat. Sci.* **59**, 313–332 (2014).
23. B. H. Mackey, M. C. Quigley, Strong proximal earthquakes revealed by cosmogenic ^{3}He dating of prehistoric rockfalls, Christchurch, New Zealand. *Geology* **42**, 975–978 (2014).
24. R. Sohbati, A. S. Murray, J. W. Borella, M. C. Quigley, OSL dating of prehistoric rockfalls, paper presented at the UK Luminescence and ESR Meeting, Scottish Universities Environmental Research Centre, University of Glasgow, Glasgow, U.K., July 2015.
25. Y. Okura, H. Kitahara, T. Sammori, A. Kawanami, The effects of rockfall volume on runout distance. *Eng. Geol.* **58**, 109–124 (2000).
26. P. Bartelt, Y. Buehler, M. Christen, Y. Deubelbeiss, C. Graf, B. W. McArdell, *RAMMS—Rapid Mass Movements Simulation: A Numerical Model for Rockfall in Research Practice, User Manual v1.5* (Institut für Schnee- und Lawinenforschung, Davos, 2013).

27. M. Christen, P. Bartelt, U. Gruber, RAMMS—A modeling system for snow avalanches, debris flows and rockfalls based on IDL. *Photogramm. Fernerkun.* **4**, 289–292 (2007).
28. L. Vick, thesis, University of Canterbury (2015).
29. H. D. Wilson, Bioclimatic zones and Banks Peninsula. *J. Canterbury Bot. Soc.* **27**, 22–29 (1993).
30. J. Shulmeister, J. M. Soons, G. W. Berger, M. Harper, S. Holt, N. Moar, J. A. Carter, Environmental and sea-level changes on Banks Peninsula (Canterbury, New Zealand) through three glaciation–interglaciation cycles. *Palaeogeogr. Palaeoclimatol. Palaeoecol.* **152**, 101–127 (1999).
31. J. M. Soons, N. T. Moar, J. Shulmeister, H. D. Wilson, J. A. Carter, Quaternary vegetation and climate changes on Banks Peninsula, South Island, New Zealand. *Global Planet. Change* **33**, 301–314 (2002).
32. D. Ackerley, A. Lorrey, J. Renwick, S. J. Phipps, S. Wagner, A. Fowler, High-resolution modelling of mid-Holocene New Zealand climate at 6000 yr BP. *Holocene* **23**, 1272–1285 (2013).
33. L. K. A. Dorren, F. Berger, A. C. Imeson, B. Maier, F. Rey, Integrity, stability and management of protection forests in the European Alps. *For. Ecol. Manage.* **195**, 165–176 (2004).
34. M. Brauner, W. Weinmeister, P. Agner, S. Vospernik, B. Hoesle, Forest management decision support for evaluating forest protection effects against rockfall. *For. Ecol. Manage.* **207**, 75–85 (2005).
35. R. I. Leine, A. Schweizer, M. Christen, J. Glover, P. Bartelt, W. Gerber, Simulation of rockfall trajectories with consideration of rock shape. *Multibody Syst. Dyn.* **32**, 241–271 (2013).
36. P. Paronuzzi, Kinematical back-analysis of block propagations for evaluating the rockfall hazard, paper presented at the 2008 Joint Meeting of The Geological Society of America, Udine, Italy, 2008.
37. A. Volkwein, K. Schellenberg, V. Labiouse, F. Agliardi, F. Berger, F. Bourrier, L. K. A. Dorren, W. Gerber, M. Jaboyedoff, Rockfall characterisation and structural protection–a review. *Nat. Hazards Earth Syst. Sci.* **11**, 2617–2651 (2011).
38. T. W. Kirkman, Statistics to use (1996), August 2015; http://www.physics.csbsju.edu/stats/.
39. M. Stuiver, H. A. Polach, Discussion reporting of ^{14}C data. *Radiocarbon* **19**, 355–363 (1977).
40. A. G. Hogg, Q. Hua, P. G. Blackwell, M. Niu, C. E. Buck, T. P. Guilderson, T. J. Heaton, J. G. Palmer, P. J. Reimer, R. W. Reimer, C. S. M. Turney, S. R. H. Zimmerman, SHCal13 Southern Hemisphere Calibration, 0–50,000 years cal BP. *Radiocarbon* **55**, 1889–1903 (2013).
41. A. R. Millard, Conventions for reporting radiocarbon determinations. *Radiocarbon* **56**, 555–559 (2014).

Acknowledgments

Funding: Financial support for the project came from the Earthquake Commission capability fund for South Island geohazards research. We thank P. C. Almond for his valuable field contributions, D. H. Bell for discussions on paleovegetation related to RAMMS modeling, and GNS Science and Christchurch City Council for Port Hills modern and pre-CES rockfall data. **Author contributions:** J.W.B. performed the field mapping and was the primary contributor to the data interpretation and preparation of the manuscript. M.Q. provided motivation for the performed field experiments and contributed to the data interpretation and preparation of the manuscript. L.V. performed RAMMS rockfall modeling and contributed to the data interpretation. **Competing interests:** The authors declare that they have no competing interests. **Data and materials availability:** All data needed to evaluate the conclusions in the paper are present in the paper and/or the Supplementary Materials. Additional data related to this paper may be requested from the authors.

Submitted 4 May 2016
Accepted 16 August 2016
Published 16 September 2016
10.1126/sciadv.1600969

Citation: J. W. Borella, M. Quigley, L. Vick, Anthropocene rockfalls travel farther than prehistoric predecessors. *Sci. Adv.* **2**, e1600969 (2016).

Anthropocene rockfalls travel farther than prehistoric predecessors

Josh Walter Borella, Mark Quigley and Louise Vick

Sci Adv **2** (9), e1600969.
DOI: 10.1126/sciadv.1600969